



Simulation Based Design of A 275kv High Voltage Bushing

* ¹Ofuase C.J. & ²Aikhoje P. T.

Department of Electrical/Electronic Engineering, Faculty of Engineering, University of Benin, Edo State, Nigeria.
prophet.aikhoje@uniben.edu¹, james.ofuase@uniben.edu²

Article Info

Keywords:

Bushing, simulation, high voltage, design

Received 06 September 2022

Revised 19 September 2022

Accepted 30 September 2022

Available online 04 Dec. 2022

<https://doi.org/10.5281/zenodo.7395698>

© 2022 NIPES Pub. All rights reserved.

Abstract

Modern bushing designs should aim at reducing the electrical stress it is subjected to, by so doing, decreasing the likelihood of partial discharge (PD) occurring. PD is the localised dielectric breakdown of small portion of an electrical insulation system under HV stress, which does not bridge the space between two conductors. In this paper, a 275kV bushing was designed using the double-sided capacitive field grading methods (radial grading and axial grading). The calculated bushing design was then modelled in COMSOL Multiphysics 4.3 (CMPH) and simulated using the electrostatic equations. The simulation results were then compared to the theoretical calculated design results. Both radial and axial grading methods allowed calculating the length and spacing between foils. These methods consider that the capacitance and voltage drop between foils is constant. The radial grading method provides a bushing design with a constant radial electric field by changing the spacing between foils. On the other hand, the axial grading methods provides a bushing design with constant axial electric field by keeping constant the difference between foil length on the air and in the oil side. In the radial grading design, the calculated and simulated radial electric field had a difference of 2.87% while there was a 4% difference in the simulated and calculated voltage drop between foils. In the axial grading design the calculated and simulated values for the voltage drop between foils was within a 32% error while the radial electric field stress was within a 20% error between the calculated and simulated value. The bushing design was improved by increasing the number of foils, which will reduce the voltage and the radial field stress. Also, reducing the length of the grounded bushing edge to be smaller than foil 21 will reduce radial field stress at the corner of the grounded bushing edge. Lastly, the foil design was modified by removing foils in the centre of the bushing and having them just along the top and bottom edges. This design would reduce the material usage per bushing thus decreasing the manufacturing cost.

1. Introduction

Bushings are typically round concentric spacers or cylinders which provide a safe, insulation interface for an electrical current to flow through electrical apparatus like transformers, switchgears, etc. When a current carrying conductor passes near any part of a material that is at earth potential, its electric field can be affected and distorted by the shape of the earthed material. Voltage from the conductor can be attracted towards the earthed material and if the electric field becomes sufficiently strong, a leakage path for the current may develop [1].

In recent years, the increase in demand for electrical energy has forced voltage levels of electrical transmission systems to be increased rapidly to reduced energy losses and improve power transfer capabilities. The need for improved bushing efficiency at a reduced cost is undoubtedly necessary with the increase in voltage levels in both AC and DC systems, since bushing failures can lead to breakdown of electrical equipment.

The various conditions under which HV equipment are operated require careful design of its insulation and the electric field profiles. This careful design of insulation in relation to dielectric stress, corona discharges and other factors help to achieve reliability and save cost on the long run. To achieve improved designs, the electric field intensities have to be controlled to avoid higher stresses that could accelerate the ageing of the insulation material [2].

An electric field is defined as the electric force per unit charge. The direction of the field is taken to be the direction of the force it would exert on a positive test charge. The dielectric field strength of an insulating material is the amount of dielectric stress the material can withstand without breakdown. Factors which influence the dielectric strength include temperature, field configurations, nature of applied voltage, surface conditions of electrodes and imperfections in dielectric material. For example, ohmic and dielectric losses produce heat which increase the overall temperature of the device and may affect its performance in the future [3].

Once the voltage distribution of a given geometry is established, the electrical stress within the bushing design is controlled to improve the efficiency of the bushing. The electrodes should be redesigned to minimize the stresses so that corona discharge is prevented. Corona discharge is an electrical discharge brought on by the ionization of a fluid surrounding a conductor that is electrically energized. The discharge will occur when the strength of the electric field around the conductor is high enough to form a conductive region, but not high enough to cause electrical breakdown or arcing to nearby objects [2]. Some studies have been carried out to minimize the issues initiated from unequal field distribution [4-9]. Hesamzadeh et al used genetic algorithms in optimizing field distribution and for the reduction of maximum field stress in 145 kV oil-impregnated paper (OIP) bushings [4]. Q. Chakravorti and H. Steinbigler used boundary element method to calculate the capacitive and resistive field of a bushing insulator [5]. A.G. Sellars and S.J. MacGregor studied a bushing for DC excitation, and aimed to control the electric field distribution by revising the geometry of the insulator [6]. Zhu Fang et. al investigated the field distribution in the inner portion of the bushing and tried to design a condenser structure [7]. Design and optimization of HV bushings using electric field computations was carried out by S. Monga et al where boundary element method based simulations was used to minimize the electric stress at some vital portions of the bushing [8]. An approach based on field emission microscopy (FEM) was used to design a bushing in [9].

This paper discusses the re-design and re-construction of a thirty year (30) old failed 275 kV HVAC bushing. Field design of HV equipment is discussed in this report along with different grading methods for AC and DC applications. Of particular note, is the double-sided capacitive grading techniques which were used to design the 275kV bushing? The 275kV bushing is designed using (1) radial grading and (2) axial grading, which form the basis of double-sided capacitive grading. The bushing consists of twenty-one (21) aluminum foils electrodes within oil impregnated paper (OIP) and is modelled in an air-oil interface. The electric field is determined with more emphasis placed on the interfaces.

2.0. Grading Methods for HV Applications

As suggested earlier, the equipotential lines that are close to the shield can cause damage in HV system (see Figure 2). It is imperative that field grading is carried out to aid insulation coordination [13].

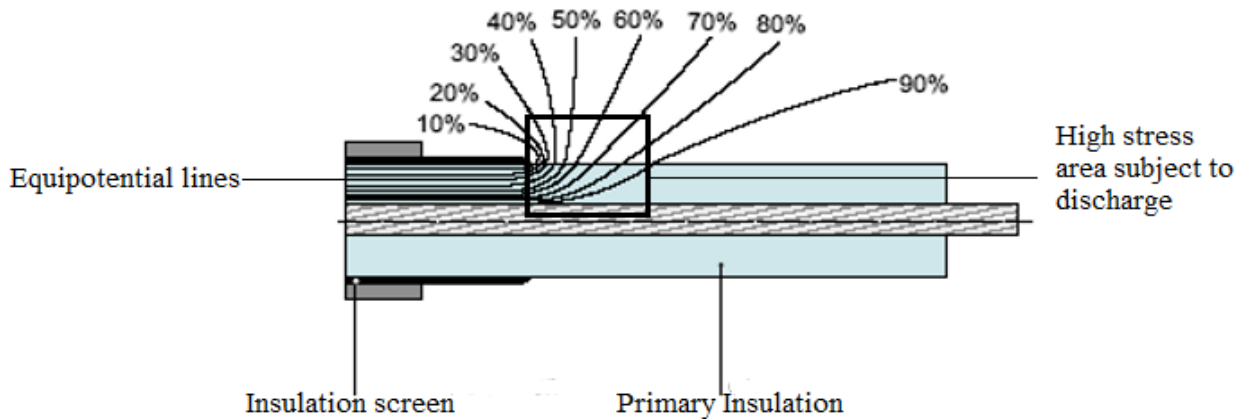


Figure 2. The Cable Termination without Stress Control [14]

In HV systems, field grading methods for decreasing stress in equipment fall into two main categories:

- a. Resistive field grading, using special materials with appropriate current-field characteristics and
- b. Capacitive field grading such as, a geometrical electrode grading with appropriate shape of conductive parts.

This simple classification is based on whether the displacement, that is, capacitive current, or resistive current dominates the field grading mechanism. [12].

Resistive field grading can produce a considerable amount of heat and is thus, not suitable for use in HV devices [13]. Capacitor grading method on the other hand utilizes high permittivity material such as electrodes in and on the insulator. Common insulator used are oil impregnated paper (OIP), oil or SF6. Here, the electrodes help reduce the concentration at the critical boundary surface as shown in Figure 3.

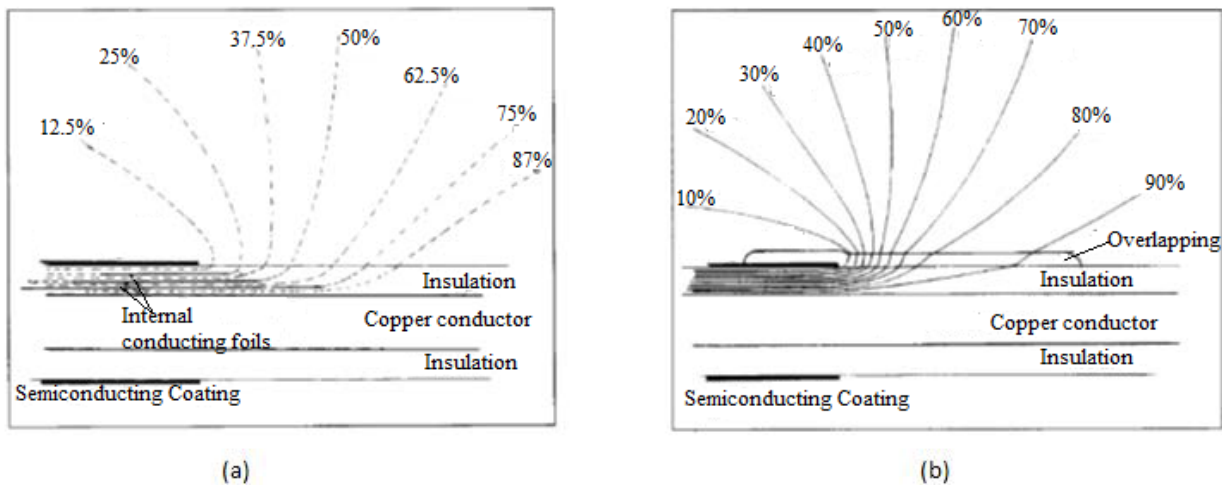


Figure 3. Effect of electrodes on the field distribution [13].

Figure 3(a) shows how the electrodes affect the electric field while 3(b) shows the electric field in same system with a layer of high permittivity material apply over the surface.

These electrodes cause certain equipotential surfaces to be set up in the field space. The use of a number of electrodes to subdivide the arrangement will result in equal partial voltages. That is to say, the insulation thickness is divided into a number of capacitors by using electrodes. These capacitors distribute voltage and the ideal voltage distribution would be linear. The parameters which control the stresses to safe level are radius of HV conductor, radius of outer layer, length of first layer, length of last layer, and system voltage [17].

2.1. Capacitive Grading

Capacitive grading for bushings is usually involves axial and radial grading since the bushing insulation is stressed both axially and radially. The capacitance-graded bushing uses conducting layers at predetermined radial intervals within the insulator (e.g. oil-impregnated paper) [13]. Figure 4 shows a representation of the equipotential lines in a basic capacitance-graded bushing. The contours of the equipotential lines show the influence of the grading elements, both radially within the core and axially along the length of the insulators [17].

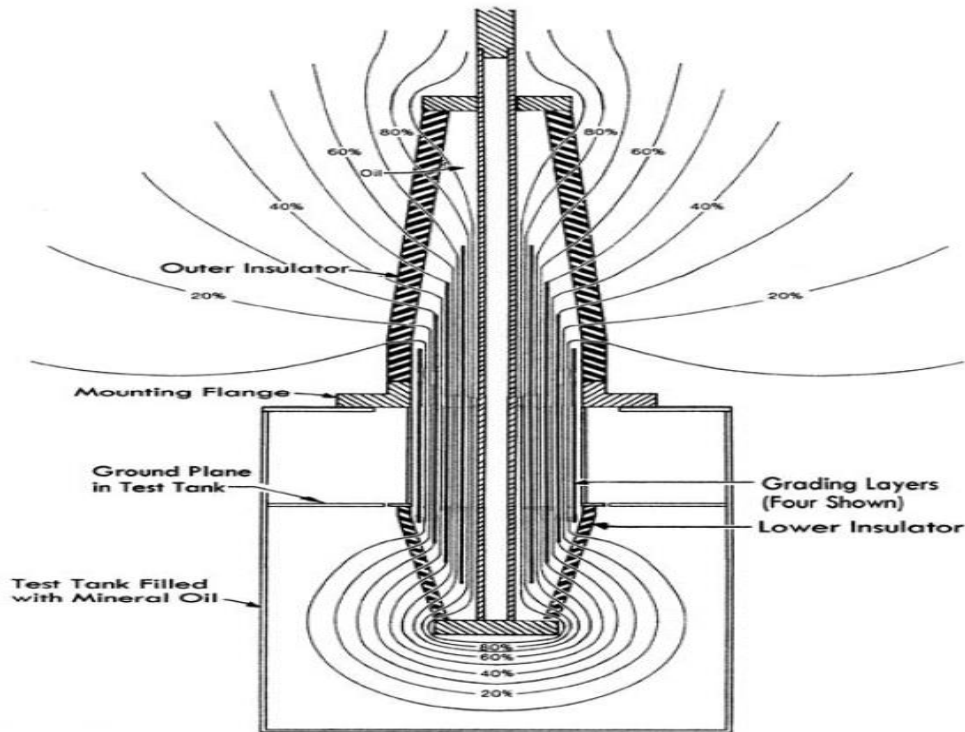


Figure 4. Equipotential lines in capacitive graded bushing [16].

Capacitive grading techniques can be subdivided into two categories: (1) double-sided capacitive grading and (2) one-sided capacitive grading. This paper focuses on the double-sided capacitive grading.

For optimum utilization of the dielectric, the capacitive grading, both for double-sided and one-sided, is arranged so the partial voltage, U , across any two adjacent layers, where N is the total number of the layers as it.

$$\Delta U = \frac{U}{N} \quad (1)$$

2.2. Double sided

Double-sided capacitive grading considers the entire bushing as a whole, notwithstanding the surrounding mediums around the bushing.

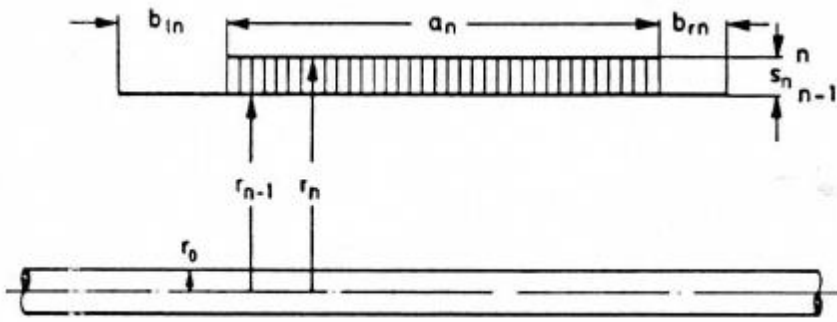


Figure 5. Foils configuration in grading field [14].

$$S_n = r_n - r_{n-1} \quad (2)$$

The capacitance between any two layers can be determined by the following equation:

$$C_n = \frac{2\pi\epsilon_0\epsilon_r a_n}{\ln \frac{r_n}{r_{n-1}}} \quad (3)$$

In *radial grading* design, the radial electric field strength, E_r is constant, when the spacing between the layers, S_n is constant and the change in voltage between each layer, ΔU is also constant. Subsequently,

$$E_r = \frac{\Delta U}{S_n} \quad (4)$$

Constant capacitance is achieved only by variation of the electrode length a_n ,

$$a_{n+1} = a_n \frac{\ln \frac{r_{n+1}}{r_n}}{\ln \frac{r_n}{r_{n-1}}} \quad (5)$$

If $S_n = r_n - r_{n-1}$ is $\ll r_n$ then;

$$a_n \approx a_{n+1} \frac{r_n}{r_{n+1}} \quad (6)$$

Axial grading requires the axial field strength to be constant such that $Ea = \frac{\Delta U}{b_n}$. This is

accomplished by displacing the layers on each side (air and oil) by the same length, that is, $b_{ln} = \text{constant} = b_l$ and $b_{rn} = \text{constant} = b_r$ and keeping the voltage between each layer, ΔU constant. Once these lengths are obtained, the length of each layer (a_n) and the spacing between each layer (s_n) can be determined from the following three equations:

$$a_{n+1} = a_n - b_l - b_r \quad (7)$$

Assuming that $C_{n+1} = C_n$:

$$\ln \frac{r_{n+1}}{r_n} = \frac{a_{n+1}}{a_n} \ln \frac{r_n}{r_{n-1}} \quad (8)$$

$$S_{n+1} \approx S_n \frac{a_{n+1}}{a_n} \frac{r_n}{r_{n-1}} \quad (9)$$

Each succeeding layer is calculated from the previous one as shown from the recursion formulae above. The flashover length is the shortest distance between the conductor and ground before electric breakdown and can be determined from the following equation;

$$L = Nb \quad (10)$$

2.3. Design of 275kV AC Bushing

Design Parameters

The schematic diagram of the initial design and other parameters are shown in Figure 6 and Table 1.

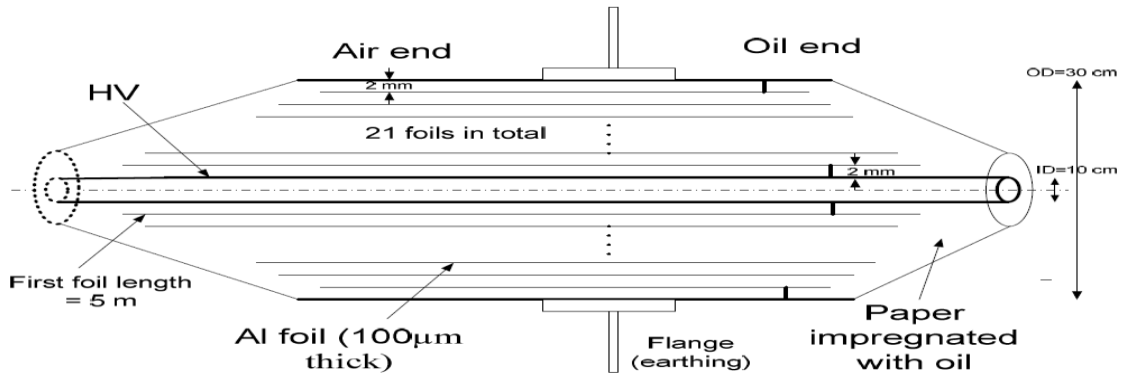


Figure 6. Schematic diagram of 275kV AC bushing (not drawn to scale) [17].

Table 1. HV bushing initial parameters

Bushing Parameters	Dimensions
Inner diameter	0.1m
Outer diameter	0.3m
First foil length (a1)	5.0m
Number of foils (N)	21
Foil thickness	0.0001

3. Design Procedure, Dimensions and Assumptions for Bushing Design

Radial design

1. The spacing, S_n between the foils were determined such that, if the 1st and 21st foils were held constant at 2mm from the conductor and flange respectively, the remaining nineteen (19) foils were evenly spaced throughout the remaining region (4.695mm apart each). Electrode radius r_n was then determined from Equation 2 for all foils.
2. The length of each of the foils, a_n , was then determined from equation 6.
3. From equation 1, $\Delta U = 13.75KV$.
4. From equation 4, the radial field stress, $E_r = 2.928kV/mm$.
5. Radial stress in OIP was assumed to be 2.5kV/mm - 4.5kV/mm [15].
6. All dielectric strengths and relative permittivity of materials used in the design are shown in Table 3 and Table 4 respectively.

Table 2. Calculated radius and foil lengths using Radial Grading Method

Electrode Number "N"	Length "an" (m)	Radius "rn" (mm)	Cn (F)
1	5	52	
2	4.57786777	56.795	9.8723E-09
3	4.221464523	61.59	9.94317E-09
4	3.916547413	66.385	1.00038E-08
5	3.652711436	71.18	1.00563E-08
6	3.422178348	75.975	1.01021E-08
7	3.219016962	80.77	1.01425E-08
8	3.038625606	85.565	1.01784E-08
9	2.877379371	90.36	1.02105E-08
10	2.732384005	95.155	1.02393E-08
11	2.60130065	99.95	1.02654E-08
12	2.482218722	104.745	1.0289E-08
13	2.373562169	109.54	1.03106E-08
14	2.274019329	114.335	1.03304E-08
15	2.182489717	119.13	1.03486E-08
16	2.098043171	123.925	1.03654E-08
17	2.019888129	128.72	1.0381E-08
18	1.94734674	133.515	1.03954E-08
19	1.879835153	138.31	1.04088E-08
20	1.816847769	143.105	1.04213E-08
21	1.757944557	147.9	1.04331E-08

Table 3. Dielectric Strength of materials

Dielectric strength	
Material	KV/m
Mineral Oil	12000
Air	3000
OIP	15000

Table 4. Relative Permittivity chart

Material	Relative Permittivity
Air	1
Aluminium Foils	10^{7+}
OIP	4.8
Oil	2.3
Copper	10^{5+}

3.1. Axial design

1. The inception voltage, U_e was assumed to be 950kV based on IEC standards [2].
2. The average field strength along the boundary surface (E_{av}) was limited to 3kV/cm at the insulation-air interface and was assumed to be four times higher (12kV/cm) at the insulation-oil interface. From equation 10, $L_{air} = 3.167m$ and $L_{oil} = 0.7917m$.
3. It was assumed that 70% of the bushing would be located in air.
4. To avoid a large gap between the 20th and 21st foil, the 2nd foil (r_2) was fixed at a certain location where $r_2 = 0.056664m$. Other electrode radii were calculated using equation 8.
5. Foil spacing was calculated with the equation 2.
6. All dielectric strengths and material permittivity are same as Tables 3 and 4.
7. All dimensions for the design and CMPH modelling are shown in Table 5 below.
8. The axial field strength was calculated as 86.84 kV/m and 347.37 kV/m in air and oil respectively.

Table 5. Calculated dimensions used in the Axial grading method

Foil Number (n)	a_n (m)	r_n (m)	s_n (m)	Capacitance (c_n) - F
0	n/a	0.05	n/a	n/a
1	5	0.052	0.002	0.0000000347
2	4.80208333	0.056664	0.004664	0.0000000156
3	4.60416667	0.06152812	0.00486412	0.0000000155
4	4.40625	0.066573684	0.005045564	0.0000000155
5	4.20833333	0.071778448	0.005204764	0.0000000155
6	4.01041667	0.077116634	0.005338186	0.0000000155
7	3.8125	0.082559033	0.005442399	0.0000000154
8	3.61458333	0.088073177	0.005514144	0.0000000154
9	3.41666667	0.093623583	0.005550406	0.0000000154
10	3.21875	0.09917207	0.005548487	0.0000000154
11	3.02083333	0.104678148	0.005506078	0.0000000153
12	2.82291667	0.110099466	0.005421318	0.0000000153
13	2.625	0.115392325	0.005292859	0.0000000153
14	2.42708333	0.120512242	0.005119917	0.0000000152
15	2.22916667	0.125414554	0.004902312	0.0000000152
16	2.03125	0.130055055	0.004640501	0.0000000152
17	1.83333333	0.134390654	0.004335599	0.0000000152
18	1.63541667	0.138380032	0.003989378	0.0000000151
19	1.4375	0.141984298	0.003604265	0.0000000151
20	1.23958333	0.145167613	0.003183316	0.0000000151
21	1.04166667	0.14789779	0.002730177	0.151

3.2. Electric Field Modelling Using Comsol Multiphysics 4.3 (Cmph)

The system consisted of the insulation, electrodes, air, oil and OIP. Each was meshed separately. Table 6 and Table 7 shows the setting of meshing for the radial and axial designs respectively.

Table 6. Meshing Parameters for the CMPH Radial Design

Meshing Area	Notes
Insulation (OIP)	Custom (Extra fine). Resolution of narrow region = 4
Electrodes	Custom (Extremely fine). Resolution of narrow region = 2. Minimum element size= 0.01 mm
Air	Predefined (Fine).
Oil	Predefined (Fine).
Conductor	Predefined (Fine).

Table 7. Meshing Parameters for the CMPH Axial Design

Meshing Area	Notes
Air	Custom (Extremely Fine); maximum element size = 0.003
Oil	Custom (Extremely Fine); maximum element size = 0.003
Copper	Custom (Finer); maximum element size = 0.002; Resolution of narrow regions = 5
Aluminium Foils	Custom (Extremely Fine); Resolution of narrow regions = 3
OIP	Predefined (Extremely Fine)

3.3. Simulation Results, and Discussion of Results for the Radial and Axial Electric Field Designs

3.3.1. Radial design vs CMPH Model

The bushing was designed using the radial grading and axial grading methods. The radial grading method hand calculation to design a bushing with a constant radial electric field was supported by the simulation. The calculated value was 2928kV/m and the average value in the simulation was 3012kV/m.

3.3.2. Electric field between the electrodes and OIP

The high permittivity value set on the aluminum foils allowed reduction in the electric field inside the electrode close to zero. Which make sense based on basic electromagnetic physics, which states that the electric field is zero inside an isolated metal, since there is no significant change in voltage. A high electric field between electrodes was expected. Inside the OIP, the electric field decreases more rapidly between foil 1 and foil 2 compared to between foil 20 and foil 21. This occurs because in the overall system the electric field is highest at the conductor and decreases in a non-linear way to ground.

3.3.3. Electric Field between OIP and Air

When the electric field in the OIP crosses the boundary to air, the electric field is increased significantly. This is due to the change of material from high permittivity to low permittivity. As seen in Figure 7a, there is an increase of electric field at the edge of the grounded bushing edge. Figure 7b shows the Contour plot scaled from 0 to 10000kV/m. In the figure it can be seen that the highest electric field occur right above the electrodes and at the point where the bushing edge (air/OIP) meets the grounded bushing edge.

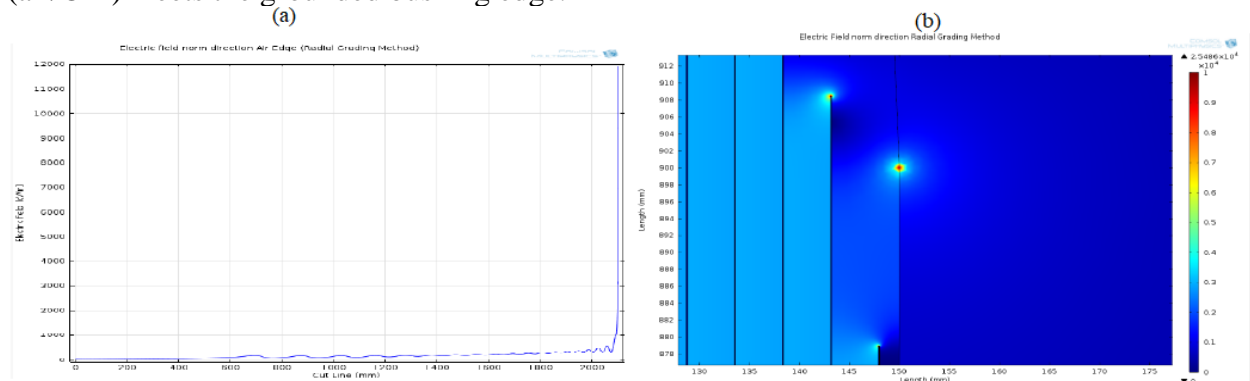


Figure 7. (a) Electric field norm direction along bushing edge, (b) Surface plot at the top edge of the bushing (air side) for the radial grading design

3.3.4. Electric Field between OIP and Oil

The electric field increases when it crosses from OIP to mineral oil. This electric field increase is less than the OIP to air situation because the permittivity of mineral oil is higher than air. The electric field is high at edge where the bushing is grounded inside the mineral oil. Figure 8 shows the contour plot scaled from 0 to 10000kV/m. It notably shows the point which experiences the highest electric field.

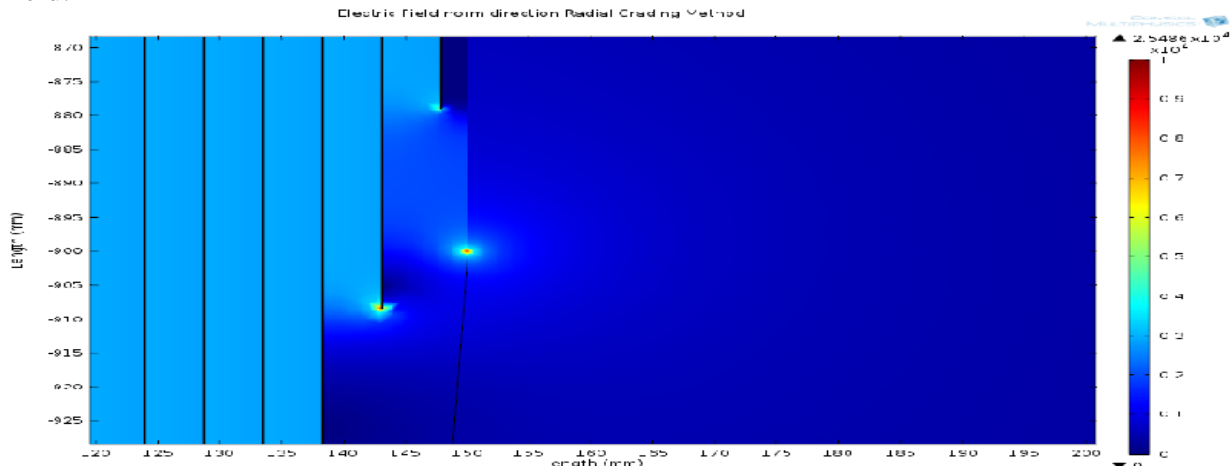


Figure 8. Surface plot at the top edge of the bushing (oil side) for the radial grading design.

3.4. Axial Design vs CMPH Model

Similar to the observations in the axial design described above, the electric field is increased significantly in OIP-air and less in OIP to oil due to the permittivity of the mediums. These results can be justified in Figure 9(a) and 9(b). The axial field strength was did not match the theoretical values as explained in Section 7.2.2, which provides a detailed discussion of the results for the axial design when compared to the CMPH modelled design.

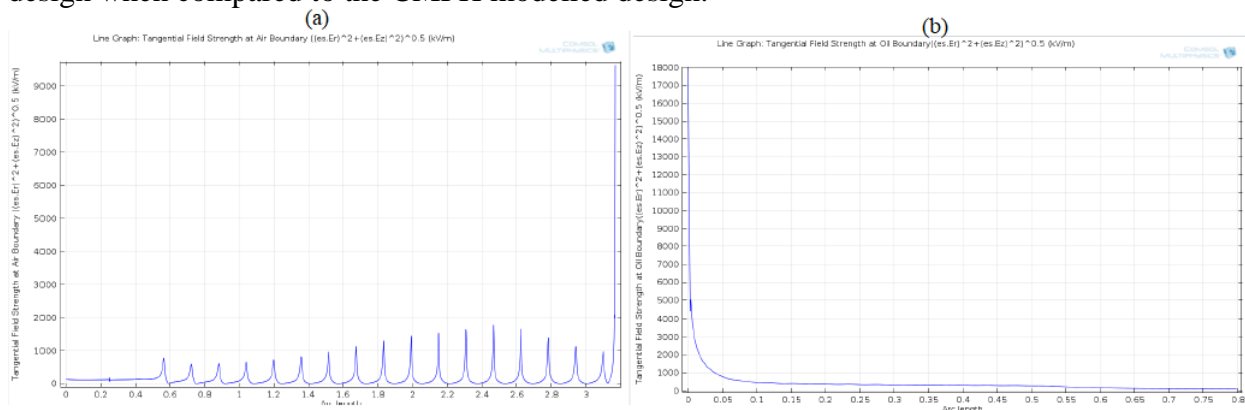


Figure 9. (a) Tangential Field Strength at Air boundary for Axial Grading Design. (b) Tangential Field Strength at Oil boundary for Axial Grading Design.

3.5. Design Optimization and Improvement of the Axial and Radial Designs

In this report, a 275 kV bushing was designed for both radial and axial capacitive grading and modelled using CMPH to simulate the electric fields. The following improvements can be made to correct the results discussed:

1. One of the solutions for improving the designs is the addition of more foil layers to bushing design to become closer to the fact that the voltage across the two layers during AC test voltage shall be about 12 kV. The addition of more layers will provide more uniform spacing, particularly in the

axial design, by reducing the large differences in spacing among the layers towards the grounded flange layer. Currently voltage across between layers is 13.75 kV but for better performance if we reduce it to 12 kV or more by adding more layers we would have better voltage profile and it would be more uniform.

2. Increasing the flashover distance in air can be one option for improving the design. This solution may increase the cost of the bushing but from a technical standpoint, the axial field strength, E_a will be reduced at the boundary.

3. Reducing length of grounded edge on bushing to be less than the length of the last foil (from A to B in figure 10) also can be one option of improving the designs. In the designs, the grounded surfaces are bigger than the length of the last foil. Applying this change would decrease the electric field at the corner of the grounded bushing edge and it would ultimately decrease electric field at the corners of the grounded bushing edge.

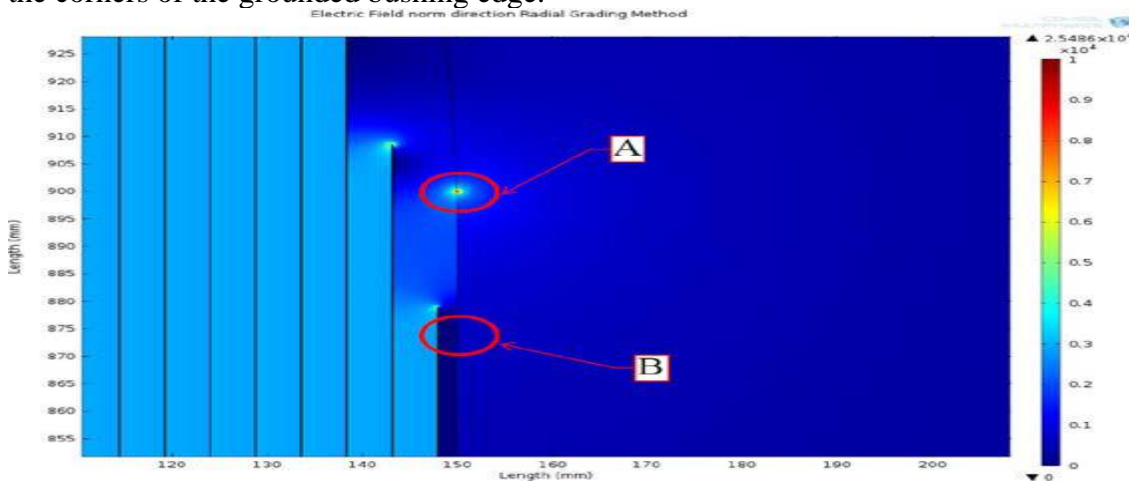


Figure 10. Changing the grounded bushing edge.

4. Another improvement is to smooth out the connection between the bushing at the interfaces at the grounded layer edge. This would reduce electric field based on the geometry.

5. Redesigning the bushing is another way to improve the design. In Figure 11, the new bushing design is shown. This option allows reducing the cost of manufacturing. This design can lead to minimum usage of material along with longer life time and higher reliability [23].

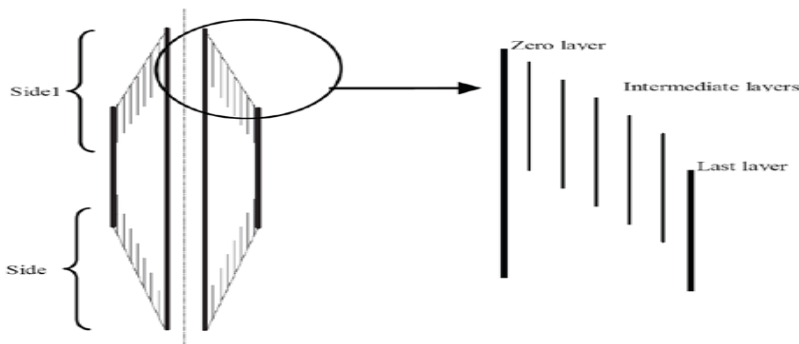


Figure 11. Conic type foil configuration [23]

4. Conclusion

In order to achieve improved designs, the electric field intensities have to be controlled to avoid the accelerated stresses which lead to ageing of the insulation material. The main parameters which control the stresses to safe levels are the radius of the conductor, radius of the outer layer, length of the first and last layer and the system voltage. The capacitive grading method utilises conducting

foils both inside and on the surface of the insulation in an attempt to spread the potential equally and are utilised in HV field designs.

In particular, double-sided capacitive grading was used to design a 275kV bushing taking into account both radial and axial stresses. Both designs allowed for calculating the lengths of the layers and the spacing between layers. The radial grading method provided a constant radial electric field by keeping the spacing between the layers constant. The electric field calculated from this design was 2928kV/m and simulated results were within 5% error due to minor variations in the voltage difference between each layer. Voltage drops between foils were also compared with theoretical results for the radial design. The calculated value was 13.75kV and the simulated value ranged from 14.25kV to 13.5kV. The axial design proved slightly more challenging and resulted large voltage drops differences between theoretical values as high as 32%. The radial field stress for the axial design, as expected was not constant due to layer spacing variations which were necessary to keep a constant capacitance between the layers. The axial field stress showed a constant field for the majority of the bushing when the range was limited between 0-500kV/m (a choice chosen primarily to compare with theoretical results); however, unlike the radial design, it was difficult to determine the axial field stress to compare with theoretical results. Both designs showed the possibility of breakdown at the grounded top layer of each bushing; however, the possibility of the bushing failing instantaneously is low. Several improvements to improve each design were highlighted. Factors such as increasing the number of foils to mitigate large voltage drops between successive layers, reducing the length of the grounded layer near the last electrode and increasing the smoothing at the edges of this surface were some of the improvements suggested to correct flaws in both designs.

References

- [1] J.P. Holtzhausen, "High voltage engineering practice and theory", W.L. Vosloo, Available at: http://www.google.co.uk/url?sa=t&rct=j&q=&esrc=s&source=web&cd=1&cad=rja&ved=0CD4QFjAA&url=http%3A%2F%2Fwww.dbc.wroc.pl%2Fcontent%2F3458%2F&ei=.75uUceO4ml0wX5oYBg&usg=AFQjCNHuaCremB3r3bl892M7rjxYoK-P4w&sig2=J2lAhZBtXw0RPqvB9UKF_g&bvm=bv.45368065.d.d2k
- [2] John Kuffel (2000), "High voltage engineering: Fundamentals", E. Kuffel, W.S. Zaengl, Second edition.
- [3] Mazen Abdel-salam, (2000) "High voltage engineering: theory and practice", Hussein Aris, Ahdab El-morshedy, Roshdy Radwan, second edition, revised and expanded.
- [4] Mohammad R. Hesamzadeh, Nasser Hosseinzadeh and Peter Wolfs, (2008) "An Advanced Optimal Approach for High Voltage AC Bushing Design", *IEEE Transactions on Dielectrics and Electrical Insulation* Vol. 15, No. 2.
- [5] S. Chakravorti, H. Steinbigler, (1998) "Capacitive-resistive Field Calculation on HV Bushings using the Boundary-element Method", *IEEE Transactions on Dielectrics and Electrical Insulation* Vol. 5 No. 2.
- [6] A G Sellars and S J MacGregor "The Design of Dielectric Barriers for HVDC Bushings, (1996) "The Institution of Electrical Engineers, published by the IEEE, Savoy Place, London.
- [7] Zhu Fang Ju Jicun Zhao Ziyu (1991) "Optimal Design of HV Transformer Bushing" Proceedings of the 3rd International Conference on Properties and Applications of Dielectric Materials, Tokyo, Japan.
- [8] S. Monga, R. S. Gorur P. Hansen and W. Massey (2006) "Design Optimization of High Voltage Bushing Using Electric Field Computations", *IEEE Transactions on Dielectrics and Electrical Insulation* Vol. 13, No. 6.
- [9] S.Ganga, M.Kanyakumari R.S.Shivakumara Aradhya, (2012) "Fem Approach to Design Functionally Graded Transformer Bushing ", *IEEE 10th International Conference on the Properties and Applications of Dielectric Materials*, Bangalore, India
- [10] M.S. Naidu, (2009) "High Voltage Engineering", Tata McGraw-Hill, New Delhi.
- [11] Grading Methods for AC/DC, Available at : http://www.google.com/url?sa=t&rct=j&q=&source=web&cd=1&cad=rja&ved=0CDIQFjAA&url=http%3A%2F%2Fwww.hst.tu-darmstadt.de%2Fuploads%2Fmedia%2Fhvt2_v_08a.pdf&ei=JEtXUeyTM6vu0gXMIIHgBw&usg=AFQjCNFaRrh2Ag8FNqDncvcqRZydvZJ0ug&bvm=bv.45373924.d.d2k
- [12] Jean P. Rivenc, (1999) "An Overview of Electrical Properties for Stress Grading Optimization", Thierry Lebey, *IEEE*, Vol. 6 No. 3.
- [13] A. ROBER, (1995) "Stress Grading for High Voltage Motor and Generator Coils", *IEEE Electrical Insulation Magazine*, Feature Article.
- [14] Dieter Kind, (1985) "High-Voltage Insulation Technology", Hermann Kärner, Vieweg and Sohn, Germany.
- [15] Shanshan (Cindy) Qin, Steven Boggs (2012) "Design Considerations for High Voltage DC Components", *IEEE Electrical Insulation Magazine*, FEATURE ARTICLE.
- [16] James H. Harlow, "Electric Power Transformer Engineering", Taylor and Francis e-Library, CRC Press LLC.
- [17] G. Chen, "Bushing Design", Available at: <https://secure.ecs.soton.ac.uk/notes/elec6089/Bushing%20design.pdf> 58
- [18] D.J Smith, (2010) "Transformer Bushing- Modelling of Electric Field and Potential Distributions within Oil Impregnated Paper with Single and Multiple Spherical Cavities", S.G. Memeekin, B.G. Stewart, P. A. Wallace, *IEEE, UPEC2010*,
- [19] W. A. Young, "An Overview of Lapp Insulator High Voltage Bushing Design", New York, Lapp Insulator Company.
- [20] M. R. Hesamzadeh, (2008) "An Advanced Optimal Approach for High Voltage AC", N. Hosseinzadeh and P. Wolfs, *IEEE*.
- [21] S. Chakravorti and H. Steinbigler, (1998) "Capacitive-resistive Field Calculation on HV Bushing using the Boundary-element Method," *IEEE Transactions on Dielectrics and Electrical Insulation*, vol. 5, no. 2, pp. 237-244.
- [22] S. Monga, R. S. Gorur, P. Hansen and W. Massey, (2006) "Design Optimization of High Voltage Bushing Using Electric Field Computations," *IEEE Transactions on Dielectrics and Electrical Insulation*, vol. 13, no. 6, p. 1217.
- [23] J. V. Champion and S. J. Dodd, (2001) "Inter-Foil Electrical Breakdown in High Voltage ERIP Condenser Bushings," *IEEE 7th International Conference on Solid Dielectric*, vol. 7, pp. 329-332.